JOTCS B
Journal of the Turkish Chemical Society
Section: B
Chemical Engineering
TURKISH CHEMICAL SOCIETY

Heterogeneous Catalysts for Biodiesel Production: Development of Bimetallic Catalysts Supported by Activated Carbon

Merve Nazlı BORAND[1]*, Başak KARAKURT ÇEVİK[1], Ezgi BAYRAKDAR ATEŞ[1]

[1]Yalova University, Energy Systems Engineering Department, Yalova, 77100, Türkiye

Abstract: This research, which explores the potential of activated carbon-supported co-impregnated metal catalysts, has the potential to significantly contribute to the field of energy systems engineering and the future of biodiesel production. In this study, spruce sawdust was used to produce activated carbon. A single-step method was applied for carbonization and activation. Spruce:KOH was adjusted as 1:2 and carbonized at 800 °C for 1 hour under nitrogen gas flow. The metal pairs were prepared with a 1:1 mass ratio for each metal. Then, 10% (w/w) metal pairs such as Cu-Fe, Fe-Zn, and Cu-Zn are impregnated on activated carbon. The catalysts were calcinated at 550 °C for 3 hours under a nitrogen atmosphere. Various characterization techniques, such as BET, SEM-EDS, and XRD analysis, were used to analyze the activity of these heterogeneous catalysts. The catalyst loading was 5% of the oil weight, the molar ratio of alcohol to oil was 19:1, the reaction temperature was 65 °C, and the reaction time was 3 hours in the esterification reaction of sunflower. According to the results, all metal pairs obtain similar FT-IR results. The biodiesel yields for Fe-Zn/AC, Cu-Zn/AC, and Cu-Fe/AC were calculated as 74.67%, 89.02%, and 68.16%, respectively.

Keywords: Biomass, biodiesel production, bimetallic catalyst, heterogeneous catalyst, activated carbon .

Submitted: July 30, 2024. **Accepted:** November 26, 2024.

Cite this: Borand, M. N., Karakurt Çevik, B., & Bayrakdar Ateş, E. (2025). Heterogeneous Catalysts for Biodiesel Production: Development of Bimetallic Catalysts Supported by Activated Carbon. Journal of the Turkish Chemical Society, Section B: Chemical Engineering, 8(1), 83–96. https://doi.org/10.58692/jotcsb.1524816

***Corresponding author. E-mail:** nazli.erdonmez@yalova.edu.tr.

1. INTRODUCTION

Due to rapid population growth and industrialization, global energy consumption increases daily, creating a critical energy crisis (Gupta & Rathod, 2019; Oyekunle et al., 2023a). Although fossil fuels now lead the energy industry, the trend towards biofuels is growing due to the depletion of fossil fuel sources and the adverse environmental effects (Karabulut et al., 2023; Monika et al., 2023; Thapa et al., 2018). On the other hand, the promotion of alternative energy sources has significantly increased over the past few decades due to growing political and societal awareness of environmental preservation and energy security. Governments, as key players in this transition, are actively promoting and investing in sustainable energy production by using biofuels instead of fossil fuels, providing reassurance and confidence in the future of energy (Chong et al., 2021; Kazıcı et al., 2021).

One of the most significant biofuels, and one whose significance is growing daily, is biodiesel (Asghari et al., 2022; Monika et al., 2023; Pacheco et al., 2022). Biodiesel is a cleaner-burning, less toxic alternative to petroleum diesel that can be used in diesel engines either in its pure form or blended with petroleum diesel (Du et al., 2018). Because of its greater flash point, biodiesel is more suited for handling and transportation. Moreover, compared to petroleum diesel, it has a better combustion emission profile with reduced emissions of carbon monoxide, particulate matter, and unburned hydrocarbons (Patle et al., 2014). Several techniques, such as micro-emulsion, pyrolysis, transesterification, and in-situ transesterification, can be used to produce biodiesel (Ahmed et al., 2023). Transesterification is the process of dispersing triglyceride and alcohol molecules, usually methanol, to replace the glycerol component with the alkyl group from the alcohol (Asghari et al., 2022). Animal fats and a

variety of vegetable oils can be used as raw materials (Li & Liang, 2017; Wahyono et al., 2022). One of the most critical factors for the transesterification reaction to proceed is catalyst addition. In the transesterification process, both homogeneous and heterogeneous catalysts are used. (Ahmed et al., 2023).

Typically, homogeneous catalysts used in oil transesterification include strong acids, strong bases, and free enzymes, such as KOH, NaOH, concentrated H_2SO_4, benzenesulfonic acid, CH_3ONa, organic amines, and microbial lipases (Xie & Li, 2023). These catalysts were selected because of their catalytic efficiency and capacity to operate in mild conditions (Angulo et al., 2020; Atadashi et al., 2013). Disadvantages of the homogeneous catalyst include the difficulties in catalyst separation, soap formation, and the use of low-free fatty acid oil (Munyentwali et al., 2022). Due to their reusability, simplicity in separation from products, and high economic efficiency, the use of heterogeneous catalysts is increasing (Fonseca et al., 2019; Jayakumar et al., 2021; Onat, Ahmet Celik, et al., 2024). The process can be run continuously because heterogeneous catalysts are simple to remove, recycle, and regenerate from the reaction. Additionally, they reduce the waste materials disposed of, avoid separation issues, and prevent soap formation. Heterogeneous catalysts have a longer lifespan, are non-corrosive, and are favorable to the environment (Dahdah et al., 2020; Oyekunle et al., 2023a; Tshizanga et al., 2017). Additionally, heterogeneous catalysts had a higher tolerance of free-fatty acid ratio and water content in the oil (Mandari & Devarai, 2022). Heterogeneous catalysts also have some drawbacks compared to homogeneous catalysts, including lower selectivity, internal mass transfer limitations, more district operation parameters, faster deactivation, longer reaction time, and the existence of big grains of catalyst (Fonseca et al., 2019; Mbaraka & Shanks, 2006; Naeem et al., 2021; Oyekunle et al., 2023a; Pandya et al., 2022; Semwal et al., 2011). Therefore, it's critical to create a stable solid catalyst and increase the stability of active species. Furthermore, the kind of oil feedstock used, operating parameters of the transesterification process, and the catalyst's active site availability all affect a heterogeneous catalyst's efficiency. The important parameters, including catalyst loading ratio, the porosity of the catalyst, the specific surface area of the catalyst, dimensions and particle size of the catalyst, calcination temperature and time, reaction time and temperatures, blending ratio, and alcohol: oil molar ratios, have a main impact on the yield and quality of the biodiesel (Ekinci & Onat, 2024; Osman et al., 2023; Oyekunle et al., 2023b). Metal hydroxides, metal complexes, metal oxides, zeolites, hydrotalcite, and supported catalysts are types of heterogeneous catalysts (Demirci et al., 2023; Şahin et al., 2020; Semwal et al., 2011). In addition, supported material is important for heterogeneous catalysts. On the other hand, the support materials offer a uniform dispersion across a greater surface area, even as they boost the stability of the catalysts. Between the support material and the active catalyst, there are adhesion contacts, van der Waals interactions, electron transfers, and distinct interphase surface structures (Hagen, 2005; Meşe et al., 2018; Onat, İzgi, et al., 2024). Support materials include a wide range of substances, including polymers, zeolites, graphene oxide, activated carbon, silica, and alumina (Abbas, 2023; Hoang et al., 2020; Onat et al., 2024; van Deelen et al., 2019).

Szkudlarek et al. performed 5%Cu–1%Ru/BEA catalyst for biodiesel production. Reaction temperature, reaction time, methanol:oil ratio, and catalyst loading were chosen as 220 °C, 2 h, 9:1, and 5%, respectively. The maximum biodiesel yield was 85.1% in these conditions (Szkudlarek et al., 2024). Farokhi and Saidi tried $NiZnFe_2O_4$, $CoZnFe_2O_4$, and $CuZnFe_2O_4$ catalysts to produce biodiesel from neem oil. According to their results maximum biodiesel yields were found 99.29% for $NiZnFe_2O_4$ catalyst (52.5 min, 16,5:1 methanol:oil ratio, 4% of catalyst loading, and 78 °C), 93% for $CoZnFe_2O_4$ catalyst (61.7 min, 19,9:1 methanol:oil ratio, 4,5% of catalyst loading, and 78°C), and 90.86% for $CuZnFe_2O_4$ catalysts (59.6 min, 21,7:1 methanol:oil ratio, 4,1% of catalyst loading, and 80°C) (Farokhi & Saidi, 2022). Kwong and Yung studied Ca and Fe catalysts for biodiesel production. The highest conversion yield was calculated as 99.5% for Ca/Fe catalyst at 1 hour reaction time, 120 °C, 20:1 of methanol:oil ratio, and 6% of catalyst loading (Kwong & Yung, 2015). Duan et al. used insect lipids to produce biodiesel. Ce-Cr/Zn catalyst was used in their study. The highest biodiesel conversion was found as 92.06% at 65 °C, 2.5% of catalyst loading, 10:1 of methanol to lipid ratio, and 8 hours of reaction time (Duan et al., 2024).

In this study, metal pairs, such as Cu-Fe, Cu-Zn, and Fe-Zn, were co-impregnated on activated carbon to produce biodiesel from sunflower oil. Sunflower oil, being an edible oil, offers consistent chemical composition and quality, which is essential for evaluating the catalytic performance of newly developed metallic catalysts. Waste oils often vary significantly in their composition due to contaminants, degradation products, and impurities, which could introduce variability and affect the interpretation of the catalytic performance. This work explores the development and use of co-impregnated metal catalysts supported by activated carbon for biodiesel synthesis, employing a novel combination of metal pairs and the supported material for the first time in the literature. The study uses activated carbon made from spruce sawdust, produced by a single carbonization and activation phase, as a support material for metal couples such as Cu-Fe, Fe-Zn, and Cu-Zn. In the esterification of sunflower oil, the study looks at these metal pairings' catalytic

effectiveness for particular reaction parameters, such as a 19:1 molar ratio of alcohol to oil, 65 °C temperature, and 5% catalyst loading. Biodiesel yields are utilized to gauge performance, and characterization methods, including BET, SEM-EDS, and XRD, are used to examine the catalysts' chemical and physical characteristics. The results of this study provide fresh information on the complementary effects of these co-impregnated metals, which are used in combination for the first time in the synthesis of biodiesel.

2. EXPERIMENTAL SECTION

2.1. Materials

Potassium hydroxide (KOH) and hydrochloric acid (HCl) were purchased from Merck, methanol (CH_3OH) and zinc nitrate hexahydrate ($Zn(NO_3)_2.6H_2O$) were purchased from Sigma-Aldrich, copper nitrate trihydrate ($Cu(NO_3)_2.3H_2O$) and iron(III) nitrate nonahydrate ($Fe(NO_3)_3.9H_2O$) were purchased from Zag Chemicals. All chemicals were used directly without any further purification, except for the spruce-derived activated carbon, which was activated before use.

2.2. Catalyst Preparation

Woody-based activated carbon was used as support material for bimetallic catalysts. Spruce wood sawdust was used as feedstock. Spruce sawdust was sieved through a 60-mesh screen (250 µm). The particles smaller than 60 mesh were used in the experiment. After sieving, spruce sawdust was dried in the oven at 104 °C for 24 h. KOH was used as an activation agent to prepare activated carbon. KOH was first dissolved in deionized water and mixed with spruce wood sawdust (2:1, weight ratio) for 24 hours and constant stirring. The mixture was then placed in an oven for 24 hours to remove the water. After drying, the mixture was subjected to calcination in a tubular furnace at 800 °C for 1 hour under nitrogen atmosphere to expand the pore size of the activated carbon. The heating rate was set as 10°C/min. After calcination in the tubular furnace, the activated carbon was washed with 0.5 M HCl to remove any residual KOH and then rinsed with deionized water until the pH reached 7. The cleaned activated carbon was then placed in an oven and dried for 24 hours. The activated support material in this study is called AC.

Co-impregnation method was used for catalyst synthesis. $Zn(NO_3)_2.6H_2O$, $Cu(NO_3)_2.3H_2O$, and $Fe(NO_3)_3.9H_2O$ were used, and the metal nitrate ratio was set as 50/50 (w/w) for each metal pair. First, two metal nitrates were dissolved in deionized water to a final concentration of 0.1 M. AC was added to this solution, with the metal nitrate to AC mass ratio set at 10%. The mixture was stirred with a magnetic stirrer for 24 hours at room temperature. Then, the solution was kept in an oven at 104 °C for 24 hours to evaporate the water. The dried catalyst was calcinated in a tubular furnace at 550 °C for 3 hours under nitrogen atmosphere, with a heating rate of 10 °C/min. After calcination, three different bimetallic catalysts were obtained. These catalysts were named as Cu-Fe/AC, Cu-Zn/AC, and Fe-Zn/AC.

2.3. Catalyst Characterization

To determine catalyst characterization, elemental analysis, Brunauer-Emmett-Teller (BET) analysis, scanning electron microscopy (SEM) and energy dispersive X-ray spectroscopy (EDS), Fourier Transform Infrared (FTIR), and X-Ray diffraction analysis (XRD) were applied. Dry sample composition was determined using an elemental analyzer (LECO CHNS-932, LECO, USA) to determine the contents of C, H, N, and S. The Quantachrome-Autosorb iQ BET analyzer (Anton Paar, Austria) was used to measure the surface area and pore structure properties of activated carbons at 77 K in the relative pressure range of 0.001 to 0.99. The samples were degassed at 180 °C for 24 hours prior to analysis. Fourier Transform Infrared (FTIR) spectra of catalysts were acquired by combining a universal attenuated total reflectance (ATR) sampling equipment with a diamond crystal with an FTIR analyzer (Perkin Elmer, USA). The 400–4000 cm^{-1} region of the spectra was collected at a resolution of 4 cm^{-1}. The surface morphologies of catalysts were examined using a scanning electron microscope (SEM) manufactured by Inspect S50 FEI Inc (USA). Using an X-ray diffractometer (Rigaku Smartlab, Japan) operating at 40 kV and 30 mA, with a scan range of 10 to 80 °C, a step width of 0.02 °C, and a scan speed of 3.035 °C/min, the X-ray diffraction (XRD) patterns of catalysts were obtained.

2.4. Transesterification of Oil

The transesterification reaction of sunflower oil and methanol was carried out in a 500-mL, three-neck, round-bottom flask equipped with a reflux condenser. The catalyst dosage was 5% of the weight of the oil, and the molar ratio of the methanol to oil was 19:1. The reaction was carried out at 65°C for 180 minutes. After completion, the catalyst was separated by filtration. The remaining liquid product, containing biodiesel and glycerol, was transferred to a separatory funnel to separate the glycerol phase at the bottom. The upper layer, biodiesel, was then rinsed in a beaker and heated at 90 °C to remove residual methanol.

The biodiesel yield was calculated using the equation below.

$\% \text{ Yield} = M_{biodiesel}/M_{oil} \times 100$

In this equation, $M_{biodiesel}$ and M_{oil} were produced biodiesel and the weight of oil used in the experiment, respectively.

3. RESULTS AND DISCUSSION

3.1. Characterization of Catalysts

3.1.1. Elemental Analysis

Elemental analysis was done to find out the content of C, H, N, and S elements in the sample. The amount of oxygen in the sample is found by subtracting the total of C, H, N, and S obtained from the elemental analysis from 100. According to elemental analysis, the spruce sawdust includes 47.59% of C, 3.50% of H, 0.00% of N, 0.00% of S, and 47.51% of O. After activation and carbonization of spruce sawdust, AC includes 92.85% of C and 7.15% of O.

3.1.2. BET analysis

Based on gas adsorption measurements, BET theory can be used to calculate the specific surface area of solid materials. This method can analyze a wide range of solid matrices, including catalyst powders and monolithic materials. BET analysis evaluates both the surface areas of catalysts and the dimensions of their pores. BET analysis was done in Autosorb iQ Station 1, the bath temperature is 77.35 K using 6 mm w/o rod cell type, with a relative pressure range of 0.001 and 0.99. It was performed after 12 hours of nitrogen desorption. The results, including the catalyst pore sizes, are detailed in Table 1.

Table 1: BET analysis results of AC and metal pairs impregnated AC.

	Surface Area(m^2/g)	**Average pore Radius (Å)**	**Total pore volume (cm^3/g)**	**Micropore volume (cm^3/g)**	**Micropore area (m^2/g)**
AC	1231.97	955.24	588.40	0.47	1113.77
Cu-Fe/AC	1269.48	937.57	595.10	0.50	1165.72
Cu-Zn/AC	1191.00	935.25	556.90	0.47	1095.76
Fe-Zn/AC	1178.59	939.51	553.70	0.46	1081.00

The analyses showed that the surface area and pore diameter were similar. This outcome is expected, as both increases during the activated carbon production from spruce sawdust. Subsequent metal adsorption is not anticipated to alter the pore diameter significantly. Cu-Zn/AC and Fe-Zn/AC slightly decreased the surface area, while Cu-Fe/AC slightly increased. Im et al. tried Cu-Fe, Cu-Ni, and Cu-Co on Al_2O_3 support, and the specific surface areas were found to be 141.3 m^2/g, 136.1 m^2/g, and 133.2 m^2/g. The highest specific surface area was Cu-Fe/ Al_2O_3 (Im et al., 2024). Alotaibi made a green synthesis Cu-Zn/zeolite catalyst in their study. Adding Cu-Zn metals to the bare zeolite support's surface significantly decreased the surface area from 252 to 165 m^2/g (Alotaibi, 2023). One possible cause of the decreased BET surface area might be the metals that have been deposited, blocking the pores in the activated carbon or accumulating on the support surface (S. Wang et al., 2023).

3.1.3. Scanning Electron Microscopy coupled with Energy Dispersion Spectroscopy (SEM-EDS) analysis

SEM-EDS analysis observes the structure of catalysts and the metals attached to them. The EDS analysis of activated carbon without metal loading is shown below.

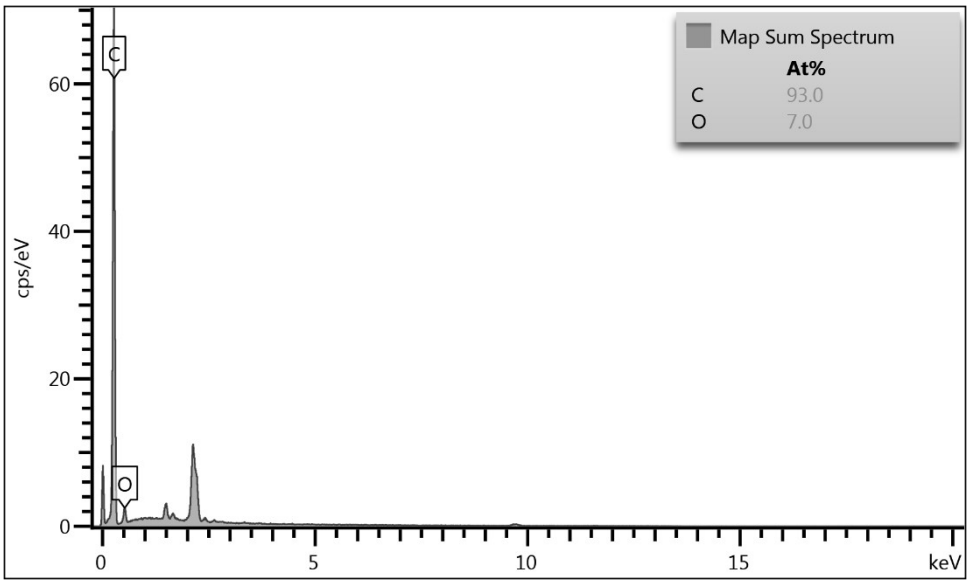

Figure 1: SEM-EDS analysis of AC.

Figure 1 shows the SEM-EDS analysis of activated carbon. No metal was detected as expected. Only carbon and oxygen content were considered. The analysis showed that the activated carbon consists of 93% carbon and 7% oxygen.

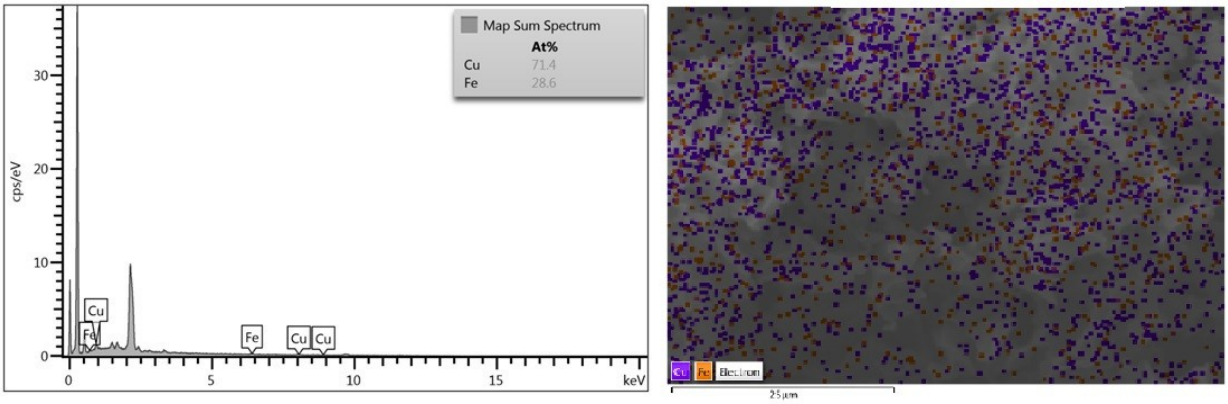

Figure 2: SEM-EDS analysis of Cu-Fe/AC.

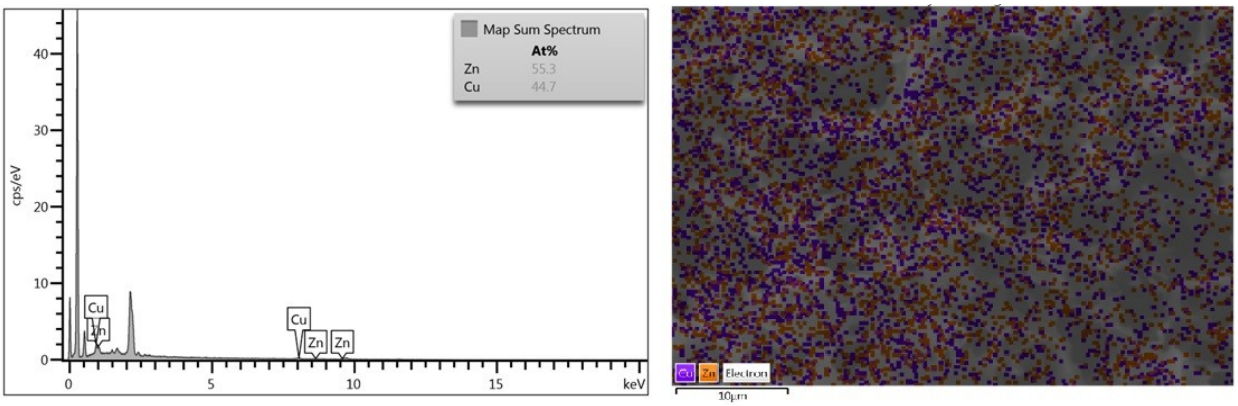

Figure 3: SEM-EDS analysis of Cu-Zn/AC.

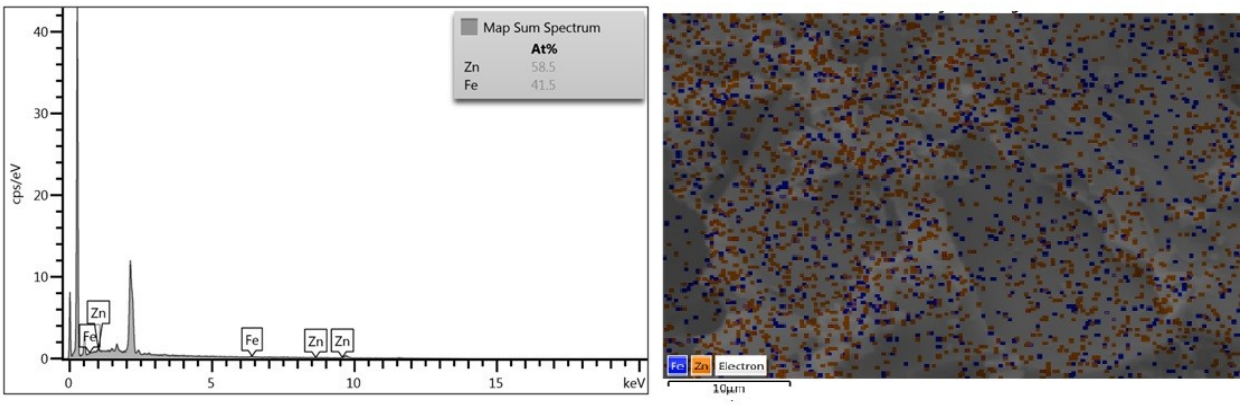

Figure 4: SEM-EDS analysis of Fe-Zn/AC.

Table 2: EDS result of Cu-Fe/AC, Cu-Zn/AC, and Fe-Zn/AC catalyst.

Catalyst	Cu (%)	Zn (%)	Fe(%)
Cu-Fe/AC	66.6		33.4
Cu-Fe/AC	77.7		22.3
Cu-Fe/AC	71.4		28.6
Cu-Zn/AC	44.7	55.3	
Cu-Zn/AC	49.9	50.1	
Cu-Zn/AC	42.9	57.1	
Fe-Zn/AC		58.6	41.4
Fe-Zn/AC		58.5	41.5
Fe-Zn/AC		56.6	43.4

Figures 2, 3, and 4 illustrate the average metal retention levels determined by the SEM-EDS method. The retention rates for the Cu-Fe/AC catalyst do not appear to be very balanced, with copper retention rates ranging from 66.6% to 77.7%. Meanwhile, iron retention ranges from 33.4% to 22.3%. Given that equal amounts of metal are loaded during catalyst production, the catalyst retains less iron relative to copper. SEM-EDS analysis of Cu-Zn/AC shows that the copper-zinc retention ratio is more evenly distributed than the iron-copper retention rate. Copper retention ranges from approximately 50.1% to 57.1%, while zinc retention ranges from 49.9% to 42.9%. The graphs show that the smoother distribution is achieved by absorbing copper and zinc into activated carbon. The Fe-Zn/AC SEM-EDS analysis yielded consistent results. The zinc retention ranges between 56.6% and 58.6%, while iron retention ranges between 43.4% and 41.4%. These results indicate that activated carbon retains less iron than zinc and copper. Bimetallic catalysts cannot have homogeneous metal contents, which may be caused by the two metals' competing adsorption during the adsorption impregnation process (Üçer et al., 2006).

SEM images present that activated carbon are irregular structures with high roughness and have visible holes and cracks, which increase specific surface area and pore volume (Bakather, 2024; Phiri et al., 2023). Dark and white sides explained the presence of the active sites in the catalyst (Q. Wang et al., 2023). When we compare the catalysts, the Cu-Fe/AC and Fe-Zn/AC catalysts show more cracks and holes, while the Cu-Zn/AC catalyst has less visible. This also explains why the surface area of the Cu-Zn/AC catalyst appears lower in the BET results.

3.1.4. X-ray diffraction (XRD) analysis

X-ray diffraction (XRD) patterns of activated carbon were obtained using a Rigaku Smartlab X-ray diffractometer which operates at 40 kV and 30 mA. The device has a scanning range of 10 to 80°, a width of 0.02°, and a scanning speed of 3.035°/min.

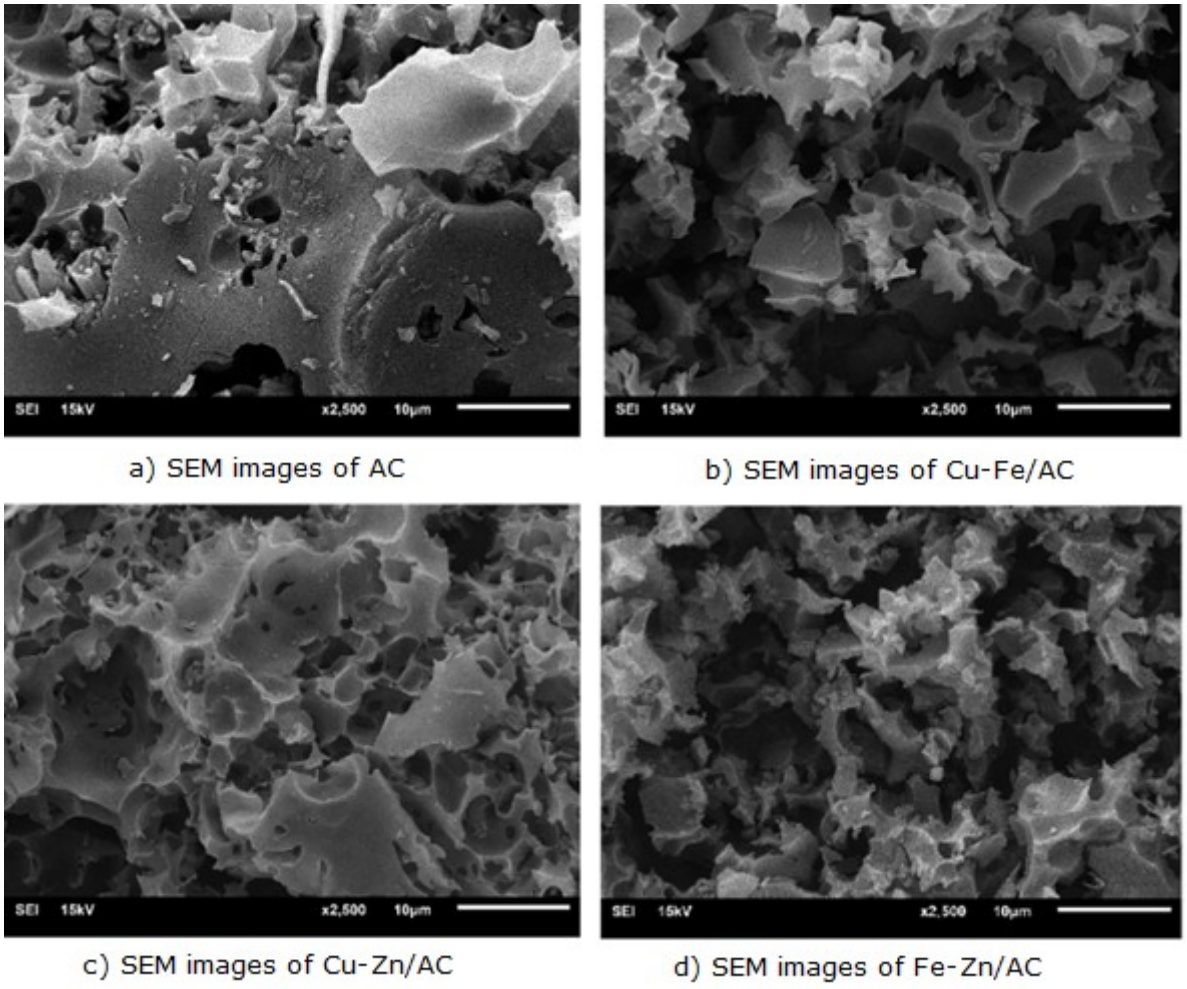

Figure 5: SEM image of catalyst (2500x).

Figure 6 presents the XRD results for both unloaded AC and metal pairs loaded ACs. Products made from activated carbon are mostly amorphous, while some crystalline material is present. The prominent XRD peaks at approximately 26° and 44° indicate an amorphous structure composed of simultaneously arranged, aromatic graphene-like sheets (Mallick et al., 2020; Mopoung & Dejang, 2021). Exhibited phases of CuO at 2θ values of 32.7°, 35.8°, 38.9°, 46.1°, 48.9°, 53.4°, 58.7°, 61.3°, 66.4° and 68.0° (JCPDS card no. #45–0937) (Bienholz et al., 2010; Charate et al., 2021) and ZnO at 2θ values of 31.9°, 34.1°, 36.7°, 47.7°, 56.5°, 62.4°, 66.59°, 68.3° and 68.92° (JCPDS card No. #36–1451) (Bel Hadj Tahar et al., 2008; Skuhrovcová et al., 2019). According to standard JCPDS card No. #22-1012, the diffraction peaks at 2θ values of 29.95°, 35.30°, 36.98°, 42.82°, 53.21°, 56.64°, 62.27° and 73.63° can be present to a cubic phase of spinel $ZnFe_2O_4$ (Iza et al., 2020). For $CuFe_2O_4$, the diffraction angles (2θ) 18.61, 30.17, 36.15, 39.01, 44.02, 54.22, and 62.39 complied with the characteristic data of JCPDS card no#034-0425 (Maleki et al., 2019).

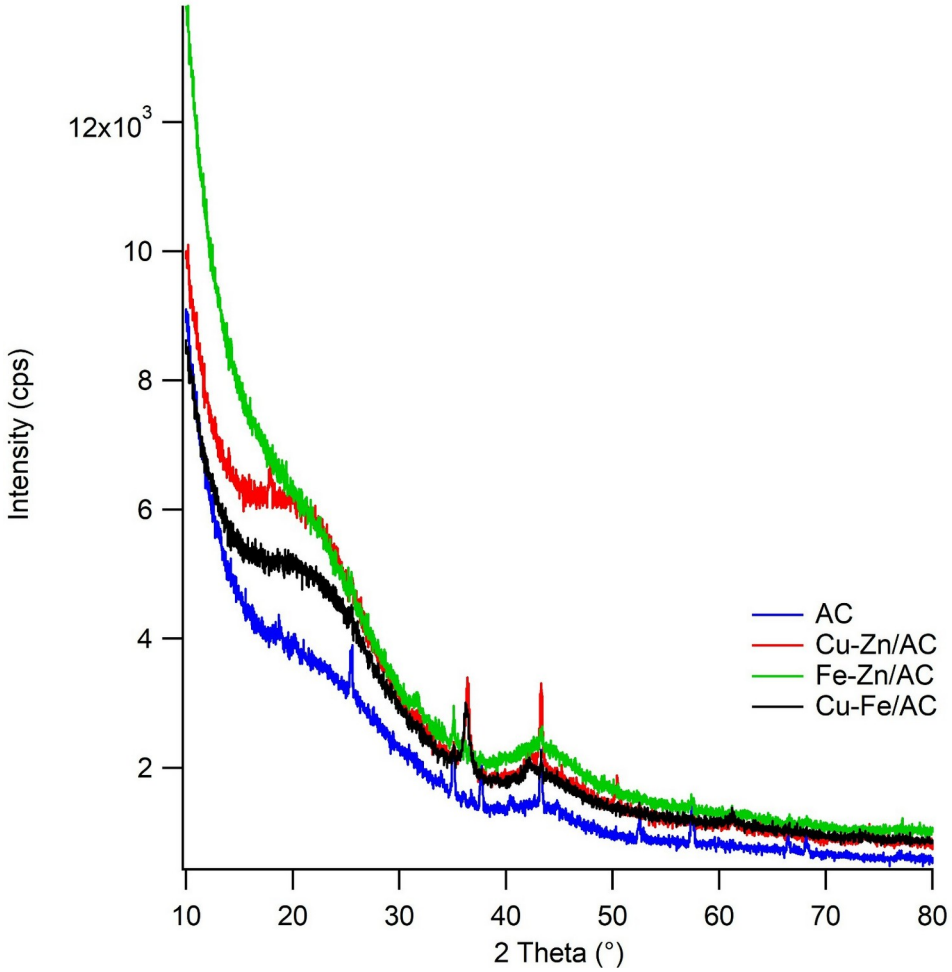

Figure 6: XRD results of catalyst.

3.2. Characterization of Biodiesel

3.2.1. FTIR results

The percentage of biodiesel in the sunflower oil transesterification reaction has been determined using the FTIR method. Samples were analyzed using Infrared mid-range in the region extending from 650-4000 cm^{-1}, which covers the absorption bands characteristic of biodiesel (methyl ester) and sunflower oil (Foroutan et al., 2022; Santiago-Torres et al., 2014). FTIR results are shown in Figure 7.

At approximately 3330 cm^{-1}, a wide vibration band declares that this structure includes O-H bonds that correspond to the presence of methanol (Santiago-Torres et al., 2014). The 3004, 2926, and 2853 cm^{-1} peaks show carboxylic acid compounds. The firm ester peaks of FTIR are around 1745 cm^{-1} (C=O bonds) and 1163-1281 cm^{-1} (C-O bonds) (Lima et al., 2022; Onat & Ekinci, 2024).The presence of these peaks confirms the occurrence of a transesterification reaction and biodiesel production. The peak at 1015 cm^{-1}, which is not present in sunflower oil, also confirms biodiesel production from sunflower oil. The green line indicates the FTIR results of sunflower biodiesel from the KOH catalyst. The biodiesel production parameters are %3 of catalyst loading, 5:1 of methanol:oil ratio, 65 °C of reaction temperature, and 90 min of reaction time. The reaction parameters are standard biodiesel production from homogeneous basic catalysts. Biodiesel production from these four catalysts seems to be similar. This indicates that the quality of the produced biodiesel is consistent across all these catalysts and this shows that the biodiesels produced with metallic catalysts are very similar in bond structure to the biodiesels produced with homogeneous basic catalysts.

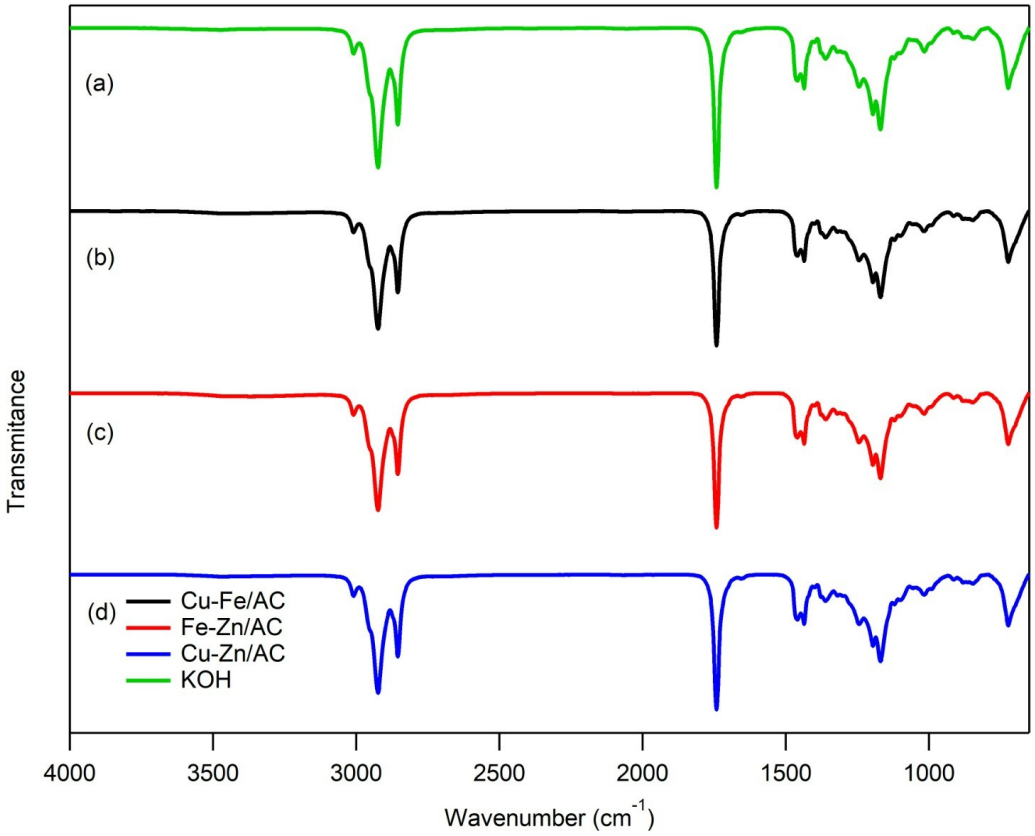

Figure 7: FTIR results of biodiesel from Cu-Fe/AC, Fe-Zn/AC, Cu-Zn/AC, and KOH catalysts.

3.3. Yield of Biodiesel

Biodiesel conversion yields are determined based on the ratio of biodiesel to oil used. In this respect, the biodiesel conversion rates for Fe-Zn/AC, Cu-Zn/AC, and Cu-Fe/AC were calculated at 74.67%, 89.02%, and 68.16%, respectively. The Cu-Zn metal pair achieves the highest conversion.

Table 3: Comparison of the biodiesel yield from sunflower oil with other literature studies.

Catalyst Type	Catalyst Ratio	Methanol:Oil Molar Ratio	Time (h)	Temp (°C)	Biodiesel Yield (%)	Reference
Ca–Mg–Al	2.5	15:1	6	60	95.00	(Dahdah et al., 2020)
CaO	3	13:1	1.66	60	94.00	(Granados et al., 2007)
K_2CO_3/alumina–silica	2	15:1	0.33	120	97.00	(Lukić et al., 2009)
Waste chalk/$CoFe_2O_4$/K_2CO_3	2.65	15.2	2.95	80	99.27	(Foroutan et al., 2022)
MgO-La_2O_3	3	18:1	5	60	97.70	(Feyzi et al., 2017)
CaO derived from sugar industry waste catalyst	5	15:1	2	60	87.64	(Bedir & Doğan, 2021)
Ca/Chicken eggshell	9	15:1	8	65	80.20	(Farooq et al., 2015)
Fe-Zn/AC	5	19:1	3	65	74.67	This study
Cu-Zn/AC	5	19:1	3	65	89.02	This study
Cu-Fe/AC	5	19:1	3	65	68.16	This study

The results show that the Cu-Zn/AC catalyst yields are consistent with literature values, whereas the other two are not. To improve conversion yields, different working conditions must be tested. As seen from the results of the SEM-EDS analysis of Cu-Zn/AC, a homogeneous distribution of the copper-zinc retention ratio and a more homogeneous structure compared to other

catalyst types effectively increased catalytic activity.

4. CONCLUSION

As a result, this study produces biomass-derived activated carbon and loads it with metal pairs to use as biodiesel conversion catalysts. Cu, Zn, and Fe were used as metals. The innovative use of spruce sawdust-derived activated carbon as a support for metal pairs such as Cu-Fe, Fe-Zn, and Cu-Zn marks a novel contribution to the literature. The results indicate that while activated carbon formation increased the surface area and pore diameter, metal impregnation did not significantly impact these properties. SEM and EDS analysis show that the metal pair Cu-Zn has the best distribution over activated carbon. A notable observation is the low iron retention across the catalysts; Fe, when paired with Cu or Zn, is less effectively retained on the activated carbon than expected. This suggests an uneven distribution of metals in the activated carbon. The highest biodiesel conversion was achieved with the Cu-Zn metal pair, reaching 89.02%, due to the nearly uniform distribution of copper and zinc on the surface. In contrast, the Cu-Fe metal pair yielded the lowest conversion rate at 68.16%. Based on these results, the effectiveness of the metal pairs in biodiesel conversion can be ranked as Cu-Zn > Fe-Zn > Fe-Cu. Despite variations in conversion yields, the biodiesel content remains consistent, indicating that all catalysts are effective for biodiesel production.

5. CONFLICT OF INTEREST

The author declares that she has no known competing financial interests or personal relationships that could have appeared to influence the work reported in this paper.

6. ACKNOWLEDGMENTS

This study was financially supported by the Research Fund of Yalova University. Project Number: 2019/AP/0015.

7. REFERENCES

Abbas, G. (2023). Metal organic framework supported surface modification of synthesized nickel/nickel oxide nanoparticles via controlled PEGylation for cytotoxicity profile against MCF-7 breast cancer cell lines via docking analysis. Journal of Molecular Structure, 1287, 135445. https://doi.org/https://doi.org/10.1016/j.molstruc.2023.135445

Ahmed, M., Ahmad, K. A., Vo, D.-V. N., Yusuf, M., Haq, A., Abdullah, A., Aslam, M., Patle, D. S., Ahmad, Z., Ahmad, E., & Athar, M. (2023). Recent trends in sustainable biodiesel production using heterogeneous nanocatalysts: Function of supports, promoters, synthesis techniques, reaction mechanism, and kinetics and thermodynamic studies. Energy Conversion and Management, 280, 116821. https://doi.org/https://doi.org/10.1016/j.enconman.2023.116821

Alotaibi, M. A. (2023). Liquid phase methanol synthesis by CO2 hydrogenation over Cu-Zn/Z catalysts: Influence of Cd promotion. Journal of the Taiwan Institute of Chemical Engineers, 153, 105210. https://doi.org/https://doi.org/10.1016/j.jtice.2023.105210

Angulo, B., Fraile, J. M., Gil, L., & Herrerías, C. I. (2020). Comparison of Chemical and Enzymatic Methods for the Transesterification of Waste Fish Oil Fatty Ethyl Esters with Different Alcohols. ACS Omega, 5(3), 1479–1487. https://doi.org/10.1021/acsomega.9b03147

Asghari, M., Hosseinzadeh Samani, B., & Ebrahimi, R. (2022). Review on non-thermal plasma technology for biodiesel production: Mechanisms, reactors configuration, hybrid reactors. Energy Conversion and Management, 258, 115514. https://doi.org/https://doi.org/10.1016/j.enconman.2022.115514

Atadashi, I. M., Aroua, M. K., Abdul Aziz, A. R., & Sulaiman, N. M. N. (2013). The effects of catalysts in biodiesel production: A review. Journal of Industrial and Engineering Chemistry, 19(1), 14–26. https://doi.org/https://doi.org/10.1016/j.jiec.2012.07.009

Bakather, O. Y. (2024). Eco-friendly biosorbent for lead removal: Activated carbon produced from grape wood. Desalination and Water Treatment, 317, 100210. https://doi.org/https://doi.org/10.1016/j.dwt.2024.100210

Bedir, Ö., & Doğan, T. H. (2021). Use of sugar industry waste catalyst for biodiesel production. Fuel, 286, 119476. https://doi.org/https://doi.org/10.1016/j.fuel.2020.119476

Bel Hadj Tahar, N., Bel Hadj Tahar, R., Ben Salah, A., & Savall, A. (2008). Effects of Individual Layer Thickness on the Microstructure and Optoelectronic Properties of Sol–Gel-Derived Zinc Oxide Thin Films. Journal of the American Ceramic Society, 91(3), 846–851. https://doi.org/https://doi.org/10.1111/j.1551-2916.2007.02221.x

Bienholz, A., Schwab, F., & Claus, P. (2010). Hydrogenolysis of glycerol over a highly active

CuO/ZnO catalyst prepared by an oxalate gel method: influence of solvent and reaction temperature on catalyst deactivation. Green Chemistry, 12(2), 290–295. https://doi.org/10.1039/B914523K

Charate, S., Shinde, S., Kondawar, S., Desai, U., Wadgaonkar, P., & Rode, C. (2021). Role of preparation parameters of Cu–Zn mixed oxide catalyst in solvent free glycerol carbonylation with urea. Journal of the Indian Chemical Society, 98(7), 100090. https://doi.org/https://doi.org/10.1016/j.jics.2021.100090

Chong, C. T., Loe, T. Y., Wong, K. Y., Ashokkumar, V., Lam, S. S., Chong, W. T., Borrion, A., Tian, B., & Ng, J.-H. (2021). Biodiesel sustainability: The global impact of potential biodiesel production on the energy–water–food (EWF) nexus. Environmental Technology & Innovation, 22, 101408. https://doi.org/https://doi.org/10.1016/j.eti.2021.101408

Dahdah, E., Estephane, J., Haydar, R., Youssef, Y., El Khoury, B., Gennequin, C., Aboukaïs, A., Abi-Aad, E., & Aouad, S. (2020). Biodiesel production from refined sunflower oil over Ca–Mg–Al catalysts: Effect of the composition and the thermal treatment. Renewable Energy, 146, 1242–1248. https://doi.org/https://doi.org/10.1016/j.renene.2019.06.171

Demirci, S., Bektaş, H., Onat, E., Şahin, Ö., Baytar, O., & İzgi, M. S. (2023). Aktif karbon destekli ucuz ve kullanışlı katalizörün amonyak bor hidrolizinde incelenmesi. Journal of Boron, 8(2), 59–65. https://doi.org/10.30728/boron.1179156

Du, E., Cai, L., Huang, K., Tang, H., Xu, X., & Tao, R. (2018). Reducing viscosity to promote biodiesel for energy security and improve combustion efficiency. Fuel, 211, 194–196. https://doi.org/https://doi.org/10.1016/j.fuel.2017.09.055

Duan, X., Yan, S., Tie, X., Lei, X., Liu, Z., Ma, Z., Wang, T., & Feng, W. (2024). Bimetallic Ce-Cr doped metal-organic frameworks as a heterogeneous catalyst for highly efficient biodiesel production from insect lipids. Renewable Energy, 224, 120128. https://doi.org/https://doi.org/10.1016/j.renene.2024.120128

Ekinci, S., & Onat, E. (2024). Activated carbon assisted cobalt catalyst for hydrogen production: synthesis and characterization. Balıkesir Üniversitesi Fen Bilimleri Enstitüsü Dergisi, 26(2), 455–471. https://doi.org/10.25092/baunfbed.1297146

Farokhi, G., & Saidi, M. (2022). Catalytic activity of bimetallic spinel magnetic catalysts (NiZnFe2O4, CoZnFe2O4 and CuZnFe2O4) in biodiesel production process from neem oil: Process evaluation and optimization. Chemical Engineering and Processing - Process Intensification, 181, 109170. https://doi.org/https://doi.org/10.1016/j.cep.2022.109170

Farooq, M., Ramli, A., & Naeem, A. (2015). Biodiesel production from low FFA waste cooking oil using heterogeneous catalyst derived from chicken bones. Renewable Energy, 76, 362–368. https://doi.org/https://doi.org/10.1016/j.renene.2014.11.042

Feyzi, M., Hosseini, N., Yaghobi, N., & Ezzati, R. (2017). Preparation, characterization, kinetic and thermodynamic studies of MgO-La2O3 nanocatalysts for biodiesel production from sunflower oil. Chemical Physics Letters, 677, 19–29. https://doi.org/https://doi.org/10.1016/j.cplett.2017.03.014

Fonseca, J. M., Teleken, J. G., de Cinque Almeida, V., & da Silva, C. (2019). Biodiesel from waste frying oils: Methods of production and purification. Energy Conversion and Management, 184, 205–218. https://doi.org/https://doi.org/10.1016/j.enconman.2019.01.061

Foroutan, R., Peighambardoust, S. J., Mohammadi, R., Peighambardoust, S. H., & Ramavandi, B. (2022). Application of waste chalk/CoFe2O4/K2CO3 composite as a reclaimable catalyst for biodiesel generation from sunflower oil. Chemosphere, 289, 133226. https://doi.org/https://doi.org/10.1016/j.chemosphere.2021.133226

Granados, M. L., Poves, M. D. Z., Alonso, D. M., Mariscal, R., Galisteo, F. C., Moreno-Tost, R., Santamaría, J., & Fierro, J. L. G. (2007). Biodiesel from sunflower oil by using activated calcium oxide. Applied Catalysis B: Environmental, 73(3), 317–326. https://doi.org/https://doi.org/10.1016/j.apcatb.2006.12.017

Gupta, A. R., & Rathod, V. K. (2019). Solar radiation as a renewable energy source for the biodiesel production by esterification of palm fatty acid distillate. Energy, 182, 795–801. https://doi.org/https://doi.org/10.1016/j.energy.2019.05.189

Hagen, J. (2005). Industrial Catalysis. Wiley. https://doi.org/10.1002/3527607684

Hoang, V. C., Dinh, K. N., & Gomes, V. G. (2020). Hybrid Ni/NiO composite with N-doped activated carbon from waste cauliflower leaves: A sustainable bifunctional electrocatalyst for efficient water splitting. Carbon, 157, 515–524. https://doi.org/https://doi.org/10.1016/j.carbon.2019.09.080

Im, Y., Muroyama, H., Matsui, T., Eguchi, K., Kim, Y., & Chae, H. (2024). Multifunctional effect of copper in bimetallic Cu-M/Al2O3 catalysts (M = Fe, Co, and Ni) for NH3 decomposition. Applied Surface Science, 669, 160396. https://doi.org/https://doi.org/10.1016/j.apsusc.2024.160396

Iza, A. M., Primadi, T. R., Ciptawati, E., Sumari, Aliyatulmuna, A., Nazriati, Suryadharma, I. B., & Fajaroh, F. (2020). Synthesis of zinc ferrite (ZnFe2O4) using microwave assisted coprecipitation method and its effectivity toward photodegradation of malachite green. AIP Conference Proceedings, 2251(1), 040025. https://doi.org/10.1063/5.0015871

Jayakumar, M., Karmegam, N., Gundupalli, M. P., Bizuneh Gebeyehu, K., Tessema Asfaw, B., Chang, S. W., Ravindran, B., & Kumar Awasthi, M. (2021). Heterogeneous base catalysts: Synthesis and application for biodiesel production – A review. Bioresource Technology, 331, 125054. https://doi.org/https://doi.org/10.1016/j.biortech.2021.125054

Karabulut, A., İzgi, M. S., Demir, H., Şahin, Ö., & Horoz, S. (2023). Optimizing hydrogen production from alkali hydrides using supported metal catalysts. Ionics, 29(5), 1975–1982. https://doi.org/10.1007/s11581-023-04962-8

Kazıcı, H. Ç., İzgi, M. S., & Şahin, Ö. (2021). A comprehensive study on the synthesis, characterization and mathematical modeling of nanostructured Co-based catalysts using different support materials for AB hydrolysis. Chemical Papers, 75(6), 2713–2725. https://doi.org/10.1007/s11696-021-01514-0

Kwong, T.-L., & Yung, K.-F. (2015). Heterogeneous alkaline earth metal–transition metal bimetallic catalysts for synthesis of biodiesel from low grade unrefined feedstock. RSC Advances, 5(102), 83748–83756. https://doi.org/10.1039/C5RA13819A

Li, J., & Liang, X. (2017). Magnetic solid acid catalyst for biodiesel synthesis from waste oil. Energy Conversion and Management, 141, 126–132. https://doi.org/https://doi.org/10.1016/j.enconman.2016.06.072

Lima, A. C., Hachemane, K., Ribeiro, A. E., Queiroz, A., Gomes, M. C. S., & Brito, P. (2022). Evaluation and kinetic study of alkaline ionic liquid for biodiesel production through transesterification of sunflower oil. Fuel, 324, 124586. https://doi.org/https://doi.org/10.1016/j.fuel.2022.124586

Lukić, I., Krstić, J., Jovanović, D., & Skala, D. (2009). Alumina/silica supported K2CO3 as a catalyst for biodiesel synthesis from sunflower oil. Bioresource Technology, 100(20), 4690–4696. https://doi.org/https://doi.org/10.1016/j.biortech.2009.04.057

Maleki, A., Hajizadeh, Z., & Salehi, P. (2019). Mesoporous halloysite nanotubes modified by CuFe2O4 spinel ferrite nanoparticles and study of its application as a novel and efficient heterogeneous catalyst in the synthesis of pyrazolopyridine derivatives. Scientific Reports, 9(1), 5552. https://doi.org/10.1038/s41598-019-42126-9

Mallick, A., Mukhopadhyay, M., & Ash, S. (2020). Synthesis, Characterization and Performance Evaluation of a Solid Acid Catalyst Prepared from Coconut Shell for Hydrolyzing Pretreated Acacia nilotica Heartwood. Journal of The Institution of Engineers (India): Series E, 101(1), 69–76. https://doi.org/10.1007/s40034-019-00153-1

Mandari, V., & Devarai, S. K. (2022). Biodiesel Production Using Homogeneous, Heterogeneous, and Enzyme Catalysts via Transesterification and Esterification Reactions: a Critical Review. BioEnergy Research, 15(2), 935–961. https://doi.org/10.1007/s12155-021-10333-w

Mbaraka, I. K., & Shanks, B. H. (2006). Conversion of oils and fats using advanced mesoporous heterogeneous catalysts. JAOCS, Journal of the American Oil Chemists' Society, 83(2), 79–91. https://doi.org/10.1007/s11746-006-1179-x

Meşe, E., Kantürk Figen, A., Coşkuner Filiz, B., & Pişkin, S. (2018). Cobalt-boron loaded thermal activated Turkish sepiolite composites (Co-B@tSe) as a catalyst for hydrogen delivery. Applied Clay Science, 153, 95–106. https://doi.org/https://doi.org/10.1016/j.clay.2017.12.008

Monika, Banga, S., & Pathak, V. V. (2023). Biodiesel production from waste cooking oil: A comprehensive review on the application of heterogenous catalysts. Energy Nexus, 10, 100209.

https://doi.org/https://doi.org/10.1016/j.nexus.2023.100209

Mopoung, S., & Dejang, N. (2021). Activated carbon preparation from eucalyptus wood chips using continuous carbonization–steam activation process in a batch intermittent rotary kiln. Scientific Reports, 11(1), 13948. https://doi.org/10.1038/s41598-021-93249-x

Munyentwali, A., Li, H., & Yang, Q. (2022). Review of advances in bifunctional solid acid/base catalysts for sustainable biodiesel production. Applied Catalysis A: General, 633, 118525. https://doi.org/https://doi.org/10.1016/j.apcata.2022.118525

Naeem, M. M., Al-Sakkari, E. G., Boffito, D. C., Gadalla, M. A., & Ashour, F. H. (2021). One-pot conversion of highly acidic waste cooking oil into biodiesel over a novel bio-based bi-functional catalyst. Fuel, 283, 118914. https://doi.org/https://doi.org/10.1016/j.fuel.2020.118914

Onat, E., Ahmet Celik, F., Şahin, Ö., Karabulut, E., & İZGİ, M. S. (2024). H2 production from ammonia borane hydrolysis with catalyst effect of Titriplex® III carbon quantum dots supported by ruthenium under different reactant Conditions: Experimental study and predictions with molecular modelling. Chemical Engineering Journal, 497, 154593. https://doi.org/https://doi.org/10.1016/j.cej.2024.154593

Onat, E., & Ekinci, S. (2024). A new material fabricated by the combination of natural mineral perlite and graphene oxide: Synthesis, characterization, and methylene blue removal. Diamond and Related Materials, 143, 110848. https://doi.org/https://doi.org/10.1016/j.diamond.2024.110848

Onat, E., İzgi, M. S., Şahin, Ö., & Saka, C. (2024). Nickel/nickel oxide nanocomposite particles dispersed on carbon quantum dot from caffeine for hydrogen release by sodium borohydride hydrolysis: Performance and mechanism. Diamond and Related Materials, 141, 110704. https://doi.org/https://doi.org/10.1016/j.diamond.2023.110704

Osman, A. I., Elgarahy, A. M., Eltaweil, A. S., Abd El-Monaem, E. M., El-Aqapa, H. G., Park, Y., Hwang, Y., Ayati, A., Farghali, M., Ihara, I., Al-Muhtaseb, A. H., Rooney, D. W., Yap, P.-S., & Sillanpää, M. (2023). Biofuel production, hydrogen production and water remediation by photocatalysis, biocatalysis and electrocatalysis. Environmental Chemistry Letters, 21(3), 1315–1379. https://doi.org/10.1007/s10311-023-01581-7

Oyekunle, D. T., Barasa, M., Gendy, E. A., & Tiong, S. K. (2023a). Heterogeneous catalytic transesterification for biodiesel production: Feedstock properties, catalysts and process parameters. Process Safety and Environmental Protection, 177, 844–867. https://doi.org/https://doi.org/10.1016/j.psep.2023.07.064

Oyekunle, D. T., Barasa, M., Gendy, E. A., & Tiong, S. K. (2023b). Heterogeneous catalytic transesterification for biodiesel production: Feedstock properties, catalysts and process parameters. Process Safety and Environmental Protection, 177, 844–867. https://doi.org/https://doi.org/10.1016/j.psep.2023.07.064

Pacheco, J. R., Villardi, H. G. D., Cavalcante, R. M., & Young, A. F. (2022). Biodiesel production through non-conventional supercritical routes: Process simulation and technical evaluation. Energy Conversion and Management, 251, 114998. https://doi.org/https://doi.org/10.1016/j.enconman.2021.114998

Pandya, H. N., Parikh, S. P., & Shah, M. (2022). Comprehensive review on application of various nanoparticles for the production of biodiesel. Energy Sources, Part A: Recovery, Utilization, and Environmental Effects, 44(1), 1945–1958. https://doi.org/10.1080/15567036.2019.1648599

Patle, D. S., Sharma, S., Ahmad, Z., & Rangaiah, G. P. (2014). Multi-objective optimization of two alkali catalyzed processes for biodiesel from waste cooking oil. Energy Conversion and Management, 85, 361–372. https://doi.org/https://doi.org/10.1016/j.enconman.2014.05.034

Phiri, J., Ahadian, H., Sandberg, M., Granström, K., & Maloney, T. (2023). The Influence of Physical Mixing and Impregnation on the Physicochemical Properties of Pine Wood Activated Carbon Produced by One-Step ZnCl2 Activation. Micromachines, 14(3), 572. https://doi.org/10.3390/mi14030572

Şahin, Ö., Bozkurt, A., Yayla, M., Kazıcı, H. Ç., & İzgi, M. S. (2020). As a highly efficient reduced graphene oxide-supported ternary catalysts for the fast hydrogen release from NaBH4. Graphene Technology, 5(3), 103–111. https://doi.org/10.1007/s41127-020-00036-y

Santiago-Torres, N., Romero-Ibarra, I. C., & Pfeiffer, H. (2014). Sodium zirconate (Na2ZrO3) as a catalyst in a soybean oil transesterification reaction for biodiesel production. Fuel

Processing Technology, 120, 34–39. https://doi.org/https://doi.org/10.1016/j.fuproc.2013.11.018

Semwal, S., Arora, A. K., Badoni, R. P., & Tuli, D. K. (2011). Biodiesel production using heterogeneous catalysts. Bioresource Technology, 102(3), 2151–2161. https://doi.org/https://doi.org/10.1016/j.biortech.2010.10.080

Skuhrovcová, L., Kolena, J., Tišler, Z., & Kocík, J. (2019). Cu–Zn–Al mixed oxides as catalysts for the hydrogenolysis of glycerol to 1,2-propanediol. Reaction Kinetics, Mechanisms and Catalysis, 127(1), 241–257. https://doi.org/10.1007/s11144-019-01560-6

Szkudlarek, Ł., Chałupka-Śpiewak, K., Maniukiewicz, W., Albińska, J., Szynkowska-Jóźwik, M. I., & Mierczyński, P. (2024). Biodiesel Production via Transesterification Reaction over Mono- and Bimetallic Copper-Noble Metal (Pt, Ru) Catalysts Supported on BEA Zeolite. Catalysts, 14(4), 260. https://doi.org/10.3390/catal14040260

Thapa, S., Indrawan, N., & Bhoi, P. R. (2018). An overview on fuel properties and prospects of Jatropha biodiesel as fuel for engines. Environmental Technology & Innovation, 9, 210–219. https://doi.org/https://doi.org/10.1016/j.eti.2017.12.003

Tshizanga, N., Aransiola, E. F., & Oyekola, O. (2017). Optimisation of biodiesel production from waste vegetable oil and eggshell ash. South African Journal of Chemical Engineering, 23, 145–156. https://doi.org/https://doi.org/10.1016/j.sajce.2017.05.003

Üçer, A., Uyanik, A., & Aygün, Ş. F. (2006). Adsorption of Cu(II), Cd(II), Zn(II), Mn(II) and Fe(III) ions by tannic acid immobilised activated carbon. Separation and Purification Technology, 47(3), 113–118. https://doi.org/https://doi.org/10.1016/j.seppur.2005.06.012

van Deelen, T. W., Hernández Mejía, C., & de Jong, K. P. (2019). Control of metal-support interactions in heterogeneous catalysts to enhance activity and selectivity. Nature Catalysis, 2(11), 955–970. https://doi.org/10.1038/s41929-019-0364-x

Wahyono, Y., Hadiyanto, H., Gheewala, S. H., Budihardjo, M. A., & Adiansyah, J. S. (2022). Evaluating the environmental impacts of the multi-feedstock biodiesel production process in Indonesia using life cycle assessment (LCA). Energy Conversion and Management, 266, 115832. https://doi.org/https://doi.org/10.1016/j.enconman.2022.115832

Wang, Q., Wang, C., Du, X., & Zhang, X. (2023). Controlled synthesis of M (M = Cr, Cu, Zn and Fe)-NiCoP hybrid materials as environmentally friendly catalyst for seawater splitting. Journal of Alloys and Compounds, 966, 171516. https://doi.org/https://doi.org/10.1016/j.jallcom.2023.171516

Wang, S., Yang, J., Wang, S., Zhao, N., & Xiao, F. (2023). Effect of Cu and Zn on the performance of Cu-Mn-Zn/ZrO2 catalysts for CO2 hydrogenation to methanol. Fuel Processing Technology, 247, 107789. https://doi.org/https://doi.org/10.1016/j.fuproc.2023.107789

Xie, W., & Li, J. (2023). Magnetic solid catalysts for sustainable and cleaner biodiesel production: A comprehensive review. Renewable and Sustainable Energy Reviews, 171, 113017. https://doi.org/https://doi.org/10.1016/j.rser.2022.113017